MDPI

Article

Characterization of the Obsidian Used in the Chipped Stone Industry in Kendale Hecala

Üftade Muşkara [1,*] and Ayşin Konak [2]

1   Department of Conservation and Restoration of Cultural Properties, Faculty of Fine Arts, Kocaeli University, İzmit 41380, Turkey
2   Department of Archaeology, Faculty of Science and Letters, Kocaeli University, İzmit 41380, Turkey; aysink@kocaeli.edu.tr
*   Correspondence: uftade.muskara@kocaeli.edu.tr

Abstract: Kendale Hecala is located on the Ambar River in the Upper Tigris Basin, province of Diyarbakır in Southeast Anatolia. Various raw materials, including obsidian, radiolarite, chert, jasper, chalcedony, and quartzite, were used in the lithic industry. Obsidian artefacts constitute an average of 64% of the chipped stone assemblage. Technological analysis reveals that obsidian was brought to the settlement as nodules and chipped into various tools at the settlement. Understanding the operational sequence of the lithic industry, chaîne opératoire, including the distribution of raw material from source to site, is important to demonstrate the socio-cultural organization of the settlement in Southeastern Anatolia during the Ubaid period. In order to identify source varieties, the obsidian artefacts uncovered from Ubaid layers of Kendale Hecala were analyzed by macro-observations, and the characterization of archaeological samples was performed using a handheld XRF. Multivariate analysis of the data indicates the use of obsidian from different resources at the settlement, including Nemrut Dağ, Bingöl B, and Group 3d.

Keywords: Upper Tigris; obsidian sourcing; pXRF; Nemrut Dağ; Group 3d; Ubaid

1. Introduction

Ubaid, which originally referred to a pottery style, characterizes the material culture that shared similar tools, architectural forms, and practices for a specific period. The distribution of the Ubaid pottery and consequently the extension of culture depending on the mutual relation between different societies approximately reached an area from the Strait of Hormuz to Northern Mesopotamia and Upper Tigris, and the Mediterranean shores [1]. The Ubaid culture spread from southern Mesopotamia to the north across Mesopotamia in the later Ubaid 3 and 4 phases, which correspond to the Northern Ubaid period, dating from about 5300 to 4500 BC [2]. The interaction within the regions is evident, especially from pottery tradition, while the obsidian circulation could also reflect the communication pattern.

The characterization studies elucidate the variety of obsidian sources reached to a specific site and obsidian procurement strategies. Determination of compositional groups will also reveal the preference for specific raw material properties for particular obsidian artefact production. The lithic chaîne opératoire was defined by Lemonnier in four stages, including extraction, reduction, production, and transformation [3,4]. Identifying the source could explain the extraction phase comprising the selection of raw material and the transportation system of obsidian [5]. On the other hand, the sequences of technical processes corresponding to the places of activity for core preparation, flake, and blade production from the core and tool kits received less recognition. The inadequate sampling strategy in provenance studies could not provide relating information.

The recent studies focused on a more systematic sampling strategy that spatially and chronologically represents the site, allowing for the detection of any possible shift in

the obsidian procurement over time. This strategy also provides insights for reduction, production, and tool finishing processes; therefore, we could obtain a more extensive perspective for (1) the lithic industry at the settlement, (2) the social and cultural structure of the society, (3) the role of the settlement in obsidian distribution, (4) the interaction between societies through trade, and (5) the spread in skill and knowledge.

In Anatolia, two major groups of geological sources are defined as Central Anatolia, including Acıgöl, Göllüdağ, Nenezidağ, Hasandağ, and Eastern Anatolia, comprising the Upper Euphrates, Lake Van, and Northeastern Anatolia regions. The previous provenance studies indicated that Bingöl B obsidians and peralkaline obsidians from Bingöl A and Nemrut Dağ were the primary sources in Southeastern Anatolia during the PPNA and PPNB (Hasankeyf, Çayönü, Hallan Çemi, and Gusir Höyük). More thorough studies that examine the geochemical data to describe obsidian selection systems and circulation networks for a period from PPN to Ubaid periods in the area detected changes in the proportions of the various geological sources over time [6–8]. Although the change could be related to the sample size, the shift in obsidian procurement and diversity of obsidian sources may suggest a modification in the taste for the physical appearances of obsidian materials, such as color, in the technology or exchange system. The effects of a shift in trade networks and centralization are reflected in the place of activity, i.e., on-site domestic production or off-site standardized blade industry [5].

In the Upper Tigris region, Kenan Tepe obsidian assemblage from Ubaid levels, for instance, suggests a difference in the production stage of obsidian tools based on their raw material [9]. Due to the proximity, the obsidian raw material diversity and *chaîne opératoire* at Kenan Tepe could bear some similarities to Kendale Hecala. However, we also acknowledge that the obsidian procurement could show regional varieties. Obsidian sources arrived at Kenan Tepe mainly include Bingöl B, Bingöl A, Nemrut Dağ, Muş, and the compositional group defined as Group 3d by Renfrew et al. [10]. The elemental composition and the physical appearance of Group 3d obsidian at the site are well described in a recent study by Campbell et al. [11]. Due to a similar proportion of Group 3d artefacts to Bingöl and Nemrut Dağ sources, the authors suggest a region between Bingöl and Nemrut Dağ for the location of Group 3d. The obsidian raw material diversity at Tell Zeidan in Northern Mesopotamia was studied by Khaldi et al. [12]. The results suggested that obsidian obtained from the Sıcaksu sub-source of Nemrut Dağ, Bingöl B, and Bingöl A were available at the site for Ubaid period contexts.

The obsidian source characterization study at Gre Fılla was conducted on fifty samples comprising various debitage and tools in 2021. The assigned origins of obsidian samples revealed that Gre Fılla was located in the distribution area of Bingöl B, Bingöl A (Solhan), and Nemrut Dağ sources [13]. While obsidian from Bingöl B constituted the majority, we could follow the temporal change in the proportions of different sources within the layers of PPNB. The archaeological evidence and C^{14} dating indicate an occupation at Gre Fılla dating from the PPNA to the late PPNB (9300–8200 cal. BC) [14]. On the other hand, the C^{14} dating at Kendale Hecala suggests a cultural sequence between 6700 and 5500 BC, including the Pottery Neolithic (PN) and the Ubaid periods. Gre Fılla and Kendale Hecala sites by the Ambar Çayı, one of the tributaries of the Upper Tigris basin, are located only 800 m. apart (Figure 1). Therefore, characterization studies at two mounds will provide valuable data to understand the obsidian procurement and exchange patterns in the region during the Neolithic and Chalcolithic periods. This study presents the elemental compositions of twenty-one obsidian artefacts from Kendale Hecala obtained from Ubaid layers using a handheld, portable X-ray fluorescence (pXRF) spectrometer. We aimed to establish the primary obsidian sources that arrived at Kendale Hecala during the Ubaid period to assign the site in the obsidian distribution system in the Upper Tigris region and define whether Group 3d obsidian was available at the site.
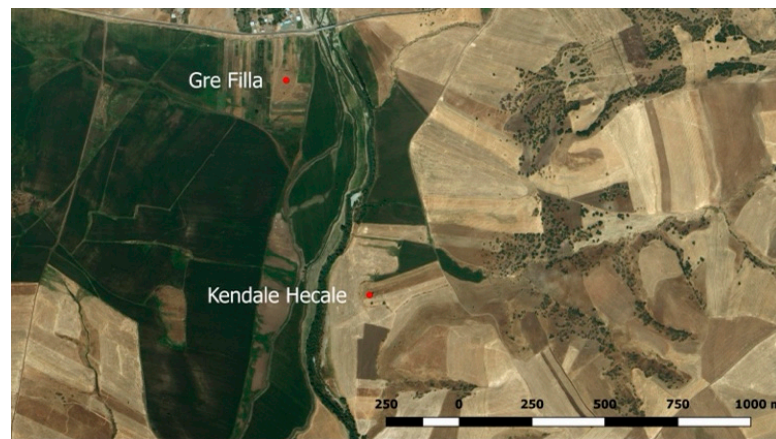
Figure 1. The aerial photography showing the locations of Gre Fılla and Kendale Hecala in the Ambar Çayı valley (Google Earth image).

2. The Archaeological Site

Ambar Dam is proposed to be constructed in the northern valley of Ambar Çayı, located in the upper Tigris valley. The salvage excavations in the region, including three mounds, Ambar Höyük, Gre Fılla, and Kendale Hecala, were initiated in 2018 by the Diyarbakır Archaeological Museum under the supervision of Prof. Dr. A. Tuba Ökse. The archaeological evidence indicates that Gre Fılla was settled from PPNA to PPNB. The site was then abandoned and used as a cemetery during the Late Antiquity and early centuries of the Middle Age. Kendale Hecala, situated at 800 m. south of Gre Fılla, is approximately 3–4 m in height, and about 0.65 ha in extent (Figures 1 and 2). According to C^{14} dating and the material remains, including pottery, lithic, and architecture, the settlement had been used in three periods spanning 6660–4540 cal. BC (Period KH III-II) and AD 500–1500 (Period KH I) (Table 1) [14,15]. Following the Early Chalcolithic settlement, the site was abandoned and reoccupied after a period of ca. 5300 years during the medieval period. The excavation at the site was sustained at ten trenches at the northern operation and four at the southern operation in the 2019 season.

Figure 2. The aerial photography of the trenches at Kendale Hecala (excavation archive).

Table 1. The cultural sequences at Kendale Hecala.

Date (BC)	Period	Pottery	Lithics	Architecture
6660–5500	KH III-PN [1]			
5500–4550	KH II-Ubaid 3–4			
500–1500 [2]	KH I-Middle Age			

[1] Pottery Neolithic. [2] AD.

3. The Lithic Industry at Kendale Hecala

The various raw materials of lithic materials consisted mainly of obsidian (65%) and other knappable siliceous rocks (35%), commonly known as flint, chert, and radiolite. Macro observations presented that the color of the obsidian materials ranges from opaque black, red-dotted black-gray, translucent green, and gray. The debitage constitutes 60% of lithic assemblage, and tools form 40%, while debris is also present. The percentage of obsidian cores (26%) is considerably lower than flint cores (74%). Bladelets, blades, and flakes comprise the major portion of the obsidian assemblage, while the exhausted obsidian cores were mainly used to produce blades and flakes based on the scares on the debitage planes. Cores with pyramidal shapes (Figure 3) or polyhedral with opposite platforms and shapeless core fragments are also defined. The lesser amount of obsidian cores and the reduction strategies (exhausted cores) suggest that obsidian was less readily available at the settlement, contrary to local knappable siliceous materials. The reason for the preference for obsidian is not apparent yet; however, it could be derived from conventional practices in the society, social aspects of the organization, or transferred skills with technology. The nodules and flakes exhibiting the primary cortex on the surfaces, along with the amount of debris, point to on-site production activity.

KH20//0068/O/01 ENV-08

Figure 3. Unipolar pyramidal blade core sample.

The length of the blades is less than 10 cm. The higher percentage of the obsidian blade and flakes, as opposed to the percentage of flint blades and flakes, may suggest that obsidian was the choice material for the production of blades and flakes. Typological classification of obsidian tools found at Kendale includes retouched blades and flakes, scrapers, splintered tools, scrapers, bores, denticulated tools, burins, notched tools, backed blades, retouched blades, and microliths (Figures 4 and 5). Furthermore, obsidian materials found at the site reflect an ad hoc flake and blade industry.

Figure 4. Retouched blade and bore samples from Kendale Hecala.

Figure 5. A retouched blade and splintered tools from Kendale Hecala.

4. Materials and Methods

4.1. Sampling

The obsidian samples were collected among 2018–2019 finds for element analysis to present the obsidian geological source variety at Kendale Hecala. All twenty-one samples are assigned to the Ubaid period and include flakes, cores, and tools such as retouched materials and scrapers (Table 2). We selected the samples to represent spatial differences at the site and followed the protocols for dimension and thickness recommended for XRF measurements [16,17]. Obsidian artefacts of various colors observed through macro analysis were selected in order to ensure our sampling strategy would reflect the raw material variety at the site. The sample morphology is an important parameter to obtain accurate and precise data when using a handheld XRF instrument. The surface roughness of the samples is one of the major limitations of archaeological studies. Irregular surfaces of archaeological samples may create an air gap between the instrument probe, resulting in a significant change in the analytical signal [18,19]. Therefore, we excluded obsidian artefacts which do not meet this requirement.

Among the sources in Eastern Anatolia, only Nemrut Dağ and Bingöl A sources were classified as peralkaline obsidians (Figure 6). Due to the proximity to Kendale Hecala, geological samples were collected from Bingöl A (Solhan) as a possible source of peralkaline obsidian artefacts found at the site. We used the geochemical data obtained by different studies using various analytical methods to compare with our dataset and to relate obsidian assemblage of Kendale Hecala to the calcalkaline obsidian sources of Bingöl B, Muş, and Süphan Dağ.

Table 2. Contextual and technological information for the analyzed Kendale Hecala II artefacts dated to cal. 5600–5000 B.C.

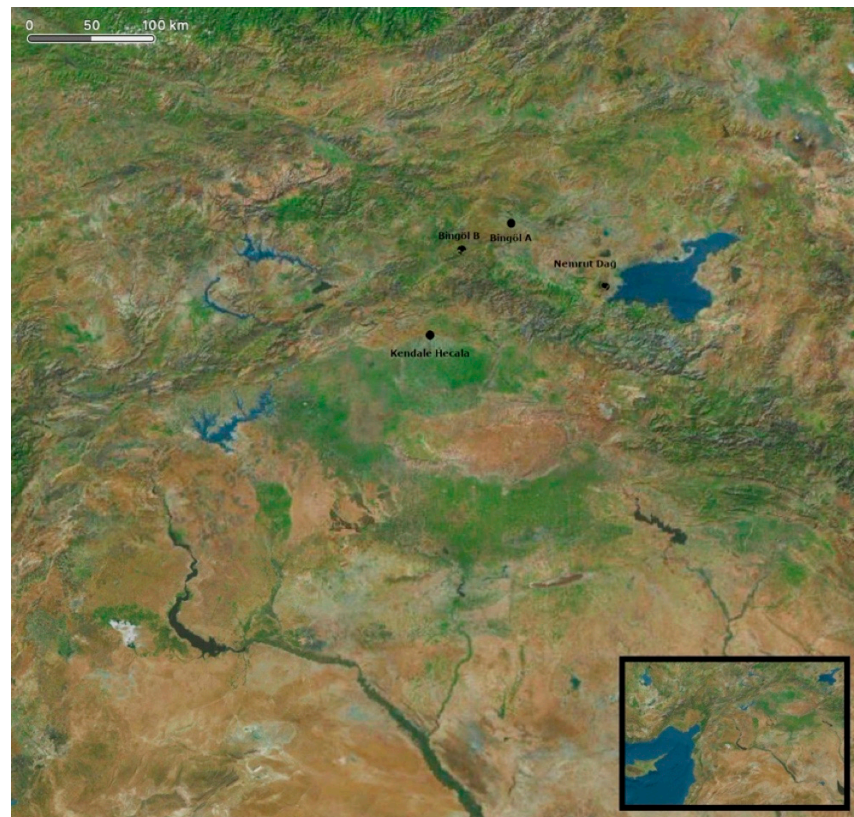| Sample Nr	Stratum	Trench	Color	Assemblage
KH-O-001	KH II	K8	Black	Retouched
KH-O-002	KH II	L8	Gray	Retouched
KH-O-003	KH II	L8	Black	Retouched
KH-O-004	KH II	L8	Gray	Retouched
KH-O-005	KH II	L8	Black	Retouched
KH-O-006	KH II	K8	Green	Retouched
KH-O-007	KH II	K8	Green	Flake
KH-O-008	KH II	K8	Green	Core
KH-O-009	KH II	K8	Green	Splitter
KH-O-010	KH II	K8	Green	Retouched
KH-O-011	KH II	K8	Green	Retouched
KH-O-012	KH II	K8	Green	Flake
KH-O-013	KH II	K8	Smokey gray	Core
KH-O-014	KH II	K8	Smokey gray	Retouched
KH-O-015	KH II	K8	Green	Core
KH-O-016	KH II	K8	Green	Flake
KH-O-017	KH II	L8	Green-gray	Flake
KH-O-018	KH II	L8	Green-gray	Retouched
KH-O-019	KH II	L8	Green-gray	Splitter
KH-O-020	KH II	L8	Black	Retouched
KH-O-021	KH II	L8	Green-gray	Retouched

Figure 6. Map showing the locations of Kendale Hecala and obsidian sources at Bingöl A, Bingöl B and Nemrut Dağ (Google Earth image).

4.2. Analytical Procedure

Chemical analysis of the obsidian samples was conducted with a handheld EDXRF; Hitachi X-Met8000 Expert. The apparatus was equipped with a silicon-drift detector (SDD) and an excitation source of X-ray tube Rh target. We use pXRF for the determination of the major elements Fe, K, Zr, Ca, and Ti, as well as the trace elements Ba, Mn, Rb, Zn, Sr, Pb, and As.

Archaeological and geological samples were cleaned with distilled water in an ultrasonic bath for 15 min. The instrument was set to 40 kV for 90 s as an optimal time. We also give at least 5 min intervals between each measurement to allow the instrument to cool and stabilize as suggested by Steiner et al. [20]. The measurements were performed according to the calibration method mentioned in Muşkara and Konak [13]. The matrixed matching strategy to check the accuracy of the calibration method requires using international standard materials (SRM or certified reference material CRM), which are generally in powdered form to ensure homogeneity. The best way to ensure appropriate validation is using the sample preparation method in the same way of reference material [21], since the comparison of the analytical signals obtained by different sample preparation methods may not always be proper (for further discussion on the issue, see [19,22]. We used East Göllüdağ obsidian samples as secondary standards to confirm the analyzer accuracy and stability before and during the analysis of the samples to ensure the validity of the calibration method for intra-laboratory comparison.

The flattest spots on the surface were selected for measurements to minimize the air gap between the sample and probe. The analysis spot size of the instrument was 5 mm, and the positioning of the analyzer was controlled by an integrated camera. All samples were analyzed in duplicate and some in triplicate to ensure the reliability of the measurements.

4.3. Data Analysis

The accuracy and reliability of obsidian provenance studies or source assignment of obsidian artefacts by pXRF have been discussed over the last decade. Various authors suggested that the data obtained by pXRF measurements can indeed be used to discriminate various geological sources. The obsidian procurement patterns at many sites in Anatolia and Near East have been usefully defined using pXRF and other portable or non-destructive devices such as SEM-EDX (scanning electron microscope-energy dispersive X-ray) PIXE (proton-induced X-ray emission), EMPA (electron micro probe analyzer). However, the concerns on the validity of pXRF measurements have not been fully addressed. The validity of pXRF has been described by Nazaroff et al. [23], referring to its ability to distinguish different geological sources, although a systematic error introduced by pXRF was observed when the results were compared with the data obtained by a lab-based XRF instrument. Two sample *t*-tests were applied between the datasets to check the accuracy of the results acquired by pXRF. K-means cluster analysis, then, was used to calculate the analytical capacity of the pXRF instrument to assign the archaeological sample to the specific source. On the other hand, a similar approach was followed by Frahm to test the validity of pXRF, although he did not apply the appropriate calibration producers, even on the artefacts that did not have the desired morphology for the measurements [24]. He concluded that "Even with systematic error from the (lack of) calibration and random error due to problematic artefacts, the compositions of these Near Eastern obsidians, as measured using HHpXRF, have greater inter-source than intra-source variations" [24] (p. 1091), expect for the peralkaline sources Nemrut Dağ and Bingöl A. However, of course, the validation of pXRF using reference materials is still required to establish accuracy and precision.

While multiple bivariate scatterplots are generally used for obsidian-source assignment, principal component analysis (PCA) has been suggested to identify compositional groups in a dataset [25–31]. In this study, we applied PCA to characterize archaeological samples and define compositional groups. The data of archaeological samples and geological samples from Bingöl A were transformed to base-10 logarithms before PCA to reduce the differences in magnitudes of the concentrations recorded and address the

skewness of the original data [32,33]. In contrast, other data-transformation methods include Z score standardization [31], multivariate Box–Cox transformation [28], and a minimum/maximum normalization [34]. PCA was performed using a correlation matrix with no rotation axis. A ratio plot of Fe/Mn vs. Rb/Zr and a ternary graph of Zr, Rb, and Zn are also used to distinguish peralkaline and calc-alkaline obsidian artefacts. In this study, multivariate statistical analysis is carried out with the help of SPSS software 28.0.1.0 (142) (IBM 2021).

5. Results

The elemental composition of geological samples originated from Bingöl A, and East Göllüdağ were reported in Muşkara and Konak [13]. Since the Ba and Sr values of Bingöl A samples acquired by pXRF was below the detection limits of the instrument, the results for the same elements originated from East Göllü Dağ obsidian samples provides insight for the lower limits of the linear dynamic range of our instrument for Ba and Sr. The element compositions of Kendale Hecala obsidian artefacts are presented in Table 3.

Table 3. Element composition of artefacts from Kendale Hecala obtained by pXRF.

Sample	Fe	Ca	Zr	Ti	Ba	Mn	Rb	Zn	Sr	Pb	As	Source
KH-O-001	12,132	4666	268	1168	317	305	192	36	38	25	5	Bingöl B
KH-O-002	12,860	7271	286	1288	318	296	208	33	39	29	3	Bingöl B
KH-O-003	15,396	7204	291	1186	419	310	203	36	38	25	6	Bingöl B
KH-O-004	12,537	8398	281	1180	373	275	194	39	37	29	1	Bingöl B
KH-O-005	12,673	5371	295	1228	431	323	205	39	38	29	3	Bingöl B
KH-O-006	28,952	2145	1148	1173	n.d. [1]	541	216	168	n.d.	34	23	Nemrut D.
KH-O-007	26,570	1791	1051	1067	n.d.	486	194	140	n.d.	31	20	Nemrut D.
KH-O-008	28,504	2342	1148	916	n.d.	500	210	167	n.d.	36	18	Nemrut D.
KH-O-009	24,063	2170	1022	899	n.d.	504	202	145	n.d.	39	22	Nemrut D.
KH-O-010	27,422	1922	1078	1149	n.d.	490	196	162	n.d.	33	17	Nemrut D.
KH-O-011	27,345	1859	892	1157	n.d.	584	194	136	n.d.	33	15	Nemrut D.
KH-O-012	24,812	1871	1042	1008	n.d.	477	206	156	n.d.	38	25	Nemrut D.
KH-O-013	10,206	5486	170	368	n.d.	331	394	74	n.d.	63	15	Group 3d
KH-O-014	11,825	3571	189	449	n.d.	430	448	84	n.d.	67	14	Group 3d
KH-O-015	11,553	4442	273	1079	356	284	198	33	34	28	4	Bingöl B
KH-O-016	30,038	2532	1260	1230	n.d.	554	229	170	n.d.	40	22	Nemrut D.
KH-O-017	18,320	2379	1082	759	n.d.	392	201	130	n.d.	31	14	Nemrut D.
KH-O-018	29,772	2807	1019	1294	n.d.	631	223	151	n.d.	42	16	Nemrut D.
KH-O-019	18,665	2587	1080	794	n.d.	408	202	142	n.d.	33	14	Nemrut D.
KH-O-020	12,158	4280	196	467	317	383	476	89	11	70	11	Group 3d
KH-O-021	33,332	2215	1098	1212	318	734	235	163	38	41	20	Nemrut D.

[1] n.d. not detected.

The log-transformed data for Fe, Zr, Ca, Ti, Mn, Rb, Zn, Pb, and As of archaeological and geological samples were used for PCA in order to distinguish various compositional groups among the Kendale artefacts. Using the scree plot and eigenvalues, two components were found significant. Examination of biplots of element vectors and the data of obsidian samples against the first and second principal components indicates four compositional groups in our dataset (Figures 7 and 8). Group 1, representing Bingöl A, is characterized by higher amounts of As and Zn. None of the archaeological samples are assigned to this group. On the other hand, Ba and Sr values found below the detection limits of the instrument and relatively higher contents of Zr and Fe identify 12 artefacts designated to Group 2 that are derived from peralkaline obsidian of Nemrut Dağ.
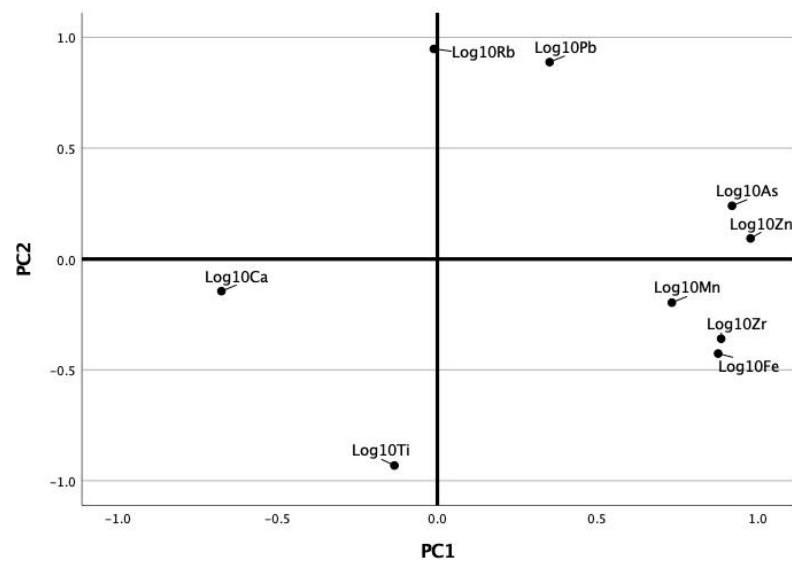
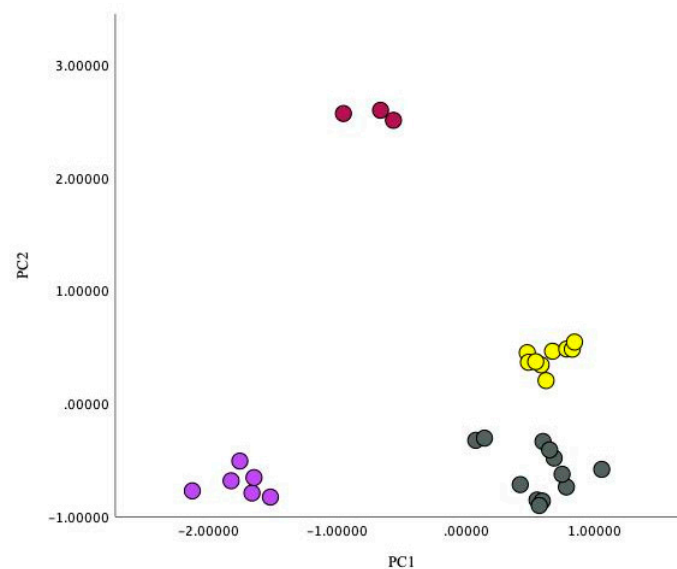**Figure 7.** Bivariate plot of loading PC1 and PC2.

Figure 8. Bivariate plot showing obsidian artefacts and Bingöl A geological samples on PC1 and PC2 for the four compositional groups (yellow circles coding Bingöl A).

The second principal component distinctively separates Group 3, including three artefacts. The discriminating positive loading of Pb and Rb elements is interesting since it suggests that these artefacts were produced from Group 3d obsidian. In a Rb vs. Pb scatterplot, which was recommended for assigning Group 3d obsidian [11], three artefacts (KH-O-013, 014, and 020) exhibit significantly higher values of Rb and Pb (Figure 9). The Pb content with a mean of 66 ± 4.54 ppm (mg/kg) obtained by Campbell et al. [11] for the artefacts defined as Group 3d is consistent with our data. The mean concentration of Rb is 439 ± 42 ppm corresponds to values that have previously been published [11,35,36], while the Rb content of KH-O-013 is relatively lower. However, it is compatible with the data of four artefacts from Yarım Tepe II obtained by Francaviglia using XRF [37] (see also [35]), and one sample from Eridu reported by Renfrew [10].
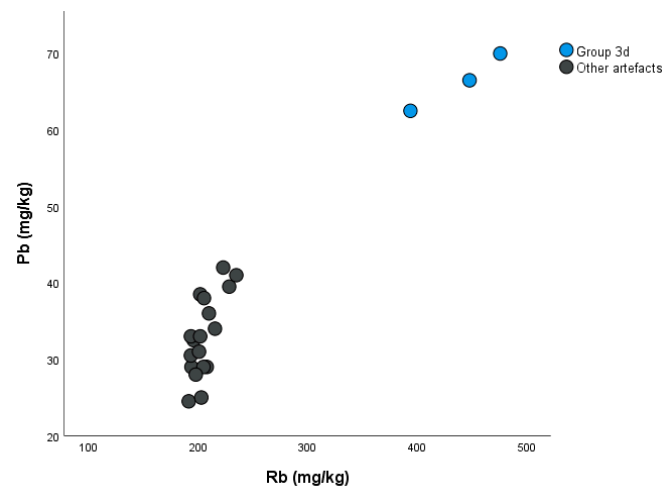
Figure 9. Rb vs. Pb scatterplot showing obsidian artefacts and Bingöl A geological samples.

Group 4, consisting of six artefacts, is separated for its higher Ca and Ti values in Figure 6. In the Ba vs. Zr scatter plot, our data for Group 4 are compared to published values in order to define the geological source of the samples (Figure 10). Group 4 artefacts have a Ba content ranging from 317 to 431 ppm, while their Zr content is between 268 and 291 ppm. Therefore, the element composition of this group corresponds to Bingöl B source.

Figure 10. Ba vs. Zr scatterplot showing Kendale Hecala obsidian artefacts (KH-O-01, 02, 03, 04, 05 and 15) and obsidian sources of Eastern Anatolia: Bingöl B (G) [38].; Bingöl B (B) [39]; Bingöl B (K) [40], Süphan Dağ (P) [41].

The Fe/Mn vs. Rb/Zr scatterplot of the samples discriminates three geochemical groups (Figure 11). One group closer to Bingöl A reference samples represents the peralkaline obsidians at Kendale Hecala; however, we understand that there is an overlapping between Nemrut Dağ obsidian, especially between Sıcaksu and Bingöl A [13]. On the contrary, the scatterplot of principal component analysis is more efficient to discriminate between two peralkaline sources. The artefacts assigned to Bingöl B are separated from peralkaline obsidian, while three artefacts identified as Group 3d appear on the upper left corner of the plot, is notably differentiated from the other artefacts. This pattern is related to a significantly higher concentration of Rb.
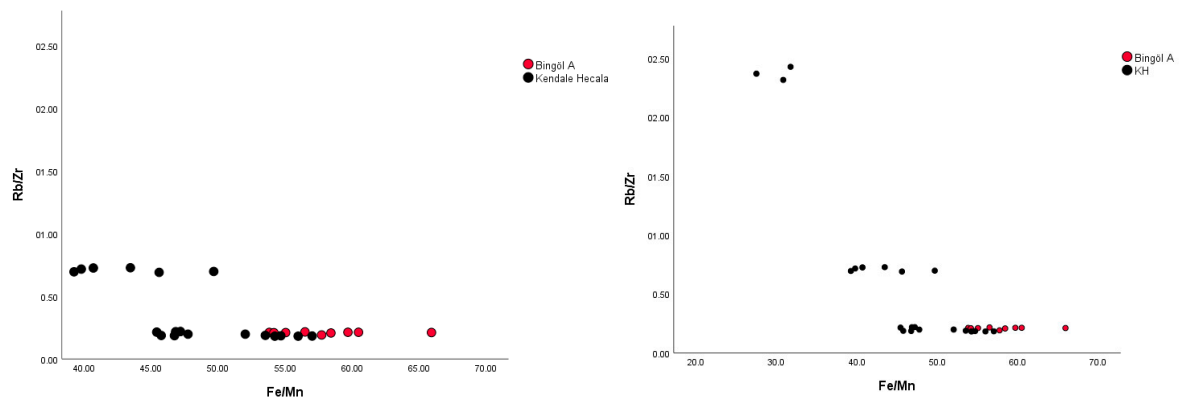
Figure 11. Bivariate plot of Fe/Mn vs. Rb/Zr showing obsidian artefacts and Bingöl A geological samples.

The compositional groups defined at Kendale Hecala are also distinguished by plotting the values of Zr, Rb, and Zn in a ternary graph (Figure 12). Most obsidian artefacts show consistencies with geological samples collected from Solhan, representing the peralkaline obsidian source. The higher Rb concentration separates three artefacts (KH-O-013, 014, and 020) and the lower values of Zn assign six artefacts (KH-O-001-005, and 015) to calcalkaline obsidians.
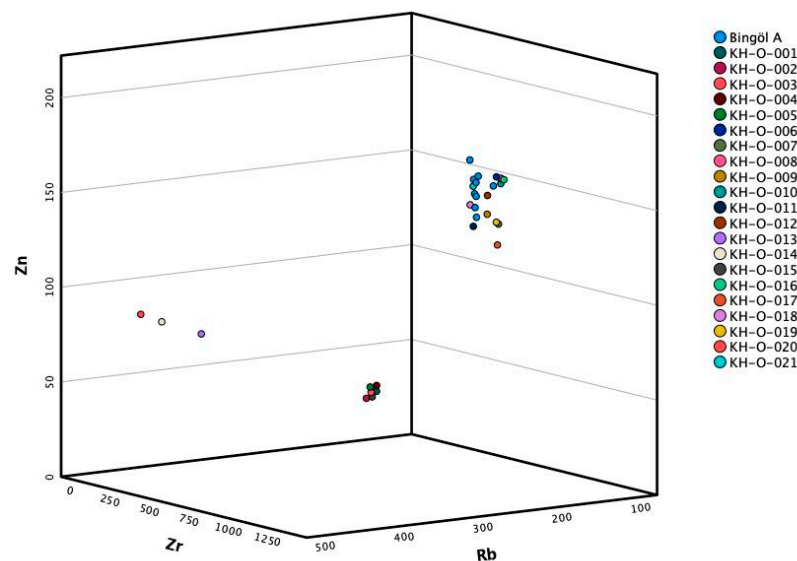

Figure 12. Ternary plot of Zr, Rb and Zn showing obsidian artefacts and Bingöl A geological samples.

6. Discussion

The geological source of 21 obsidian artefacts, including cores, flakes, retouched materials, and scrapers, were determined as Bingöl B, Nemrut Dağ, and Group 3d. Since our geological sampling represents only Bingöl A source obtained from Solhan, we applied a principal component analysis for the discrimination of different compositional groups. The total variance explained by the first and second components is 82%. The first component is positively correlated with Zn and As, while also less correlated with other components (Table 4). The second component is positively correlated with Rb and negatively correlated with Ti.

Table 4. The component matrix of PCA.

	1	2	3
Log10Fe	0.878	−0.426	0.165
Log10Zr	0.887	−0.359	−0.188
Log10Ca	−0.675	−0.145	0.644
Log10Ti	−0.134	−0.931	0.251
Log10Mn	0.733	−0.196	0.596
Log10Rb	−0.011	0.948	0.269
Log10Zn	0.979	0.093	0.000
Log10Pb	0.351	0.888	0.223
Log10As	0.921	0.240	−0.025

The PC1 separates Group 1, Group 2 (peralkaline), and Group 4 (calc-alkaline) obsidians, and PC2 discerns Group 3. On the other hand, discriminating Bingöl A and Nemrut Dağ compositional group has been difficult, especially when the data were acquired by pXRF. Various binary diagrams, including La vs. Nb and Zr vs. Nb, were applied by Chataigner [42]. Although Bingöl A and Nemrut Dağ sources are represented homogeneously, she suggests that flow dating could provide better results when archaeological samples are not allocated to either source precisely. Other quantitative analysis methods of the data have been applied, such as ratio plot of Nb/Pb vs. Y/Nb [30], Fe vs. Zr [12], or Al_2O_3 vs. FeO(T) vs. Zr [43]. Characterization studies have also identified sub-sources in Nemrut Dağ [29,42–44]. Among the defined outcrops, Sıcaksu obsidian has the most similar geochemical compositional to Böngöl A, while it was reported as the most available source at settlements in Northern Mesopotamia from the Late Neolithic to Chalcolithic period [12,29]. However, Frahm [43] argued that other than Sıcaksu, three other Nemrut sub-sources occurred at Körtik Tepe, Domuztepe, and Tell Mozan. Our data for Gre Fılla artefacts also suggest that obsidian raw material from various outcrops of Nemrut Dağ (especially Sıcaksu and Kayacık) arrived at the settlement [13].

The scatterplot of PC1 and PC2 in this study identifies peralkaline obsidians; however, archaeological samples differentiate from Bingöl A geological samples due to similar behavior of Zn-As (positive loading for Bingöl A) and Fe-Zr elements (positive loading for archaeological samples). Due to the clear separation between the groups, Group 2 artefacts are assigned to Nemrut Dağ, although no overlapping regions may have resulted from the number of archaeological samples analyzed. On the other hand, the representation of the sample on the bivariate plot of Fe/Mn vs. Rb/Zr supports the allocation of obsidian artefacts to Nemrut Dağ. Future studies will include obsidian samples from Sıcaksu, Kayacık, and other outcrops of Nemrut Dağ in order to test the efficiency of the variable set used in the principal component analysis. While Fe, Zr, and Zn have been used for identifying peralkaline obsidians, As appears to be among the set of discriminating variables.

The Group 3d obsidian compositional group was initially defined by Renfrew et al. [10]. Various obsidian sources, including Central Anatolia, Eastern Anatolia, and Armenia, were analyzed in this study using OES (optical emission spectroscopy) instrument. After appointing four distinct compositional groups, they specified the chemical characteristics of Group 3d as: "Two specimens that fall in group 3c on the barium-zirconium graph (nos. 171, Ras Shamra, and 235, Dahran) have been distinguished as Group 3d, on the basis of an exceptionally high content of rubidium and lithium. It is not yet clear whether these are from an otherwise undocumented source, possibly in Armenia, or are anomalous analyses from known sources" [10] (p. 33). The most recent study on Group 3d is published by Campbell et al. [11]. Although the main focus was the artefacts recovered from Kenan Tepe, they provide a comprehensive description of the physical and geochemical properties of Group 3d obsidian. They suggest a scatter plot of a Rb vs. Pb is the most accurate method for identification of this type of raw material since the concentrations of these elements are significantly higher. The previous studies and Kenan Tepe data provide consistent result for the elements that define for Group 3d. The mean concentration of Rb is reported to be

higher than 450 ppm, and the Pb content is around 60 ppm. Other than Rb and Pb, the authors mentioned that the concentrations of Li, B, and Cs could be distinctive for this group. In our dataset, we assigned three artefacts, KH-O-013 (core), KH-O-014 (retouched), and KH-O-020 (retouched), to Group 3d.

Kenan Tepe is the only settlement so far that the large-scale use of this compositional group has been detected [11]. Due to the intensive use of Group 3d and on-site production, the authors proposed a possible location of Group 3d as more accessible to Kenan Tepe, probably between Nemrut Dağ and Bingöl area. When we compare the proportion of Group 3d artefact among the other sources, the ratio of Group 3d artefacts is 14% (Figure 13). On the other hand, obsidian assemblage at the site indicates on-site production, regardless of obsidian type. However, the number of obsidian artefacts was limited in our study since the sampling was undertaken at the earlier stages of the excavation. Future studies will produce data to better understand the obsidian chaîne opératoire at Kendale Hecala during the Ubaid period.
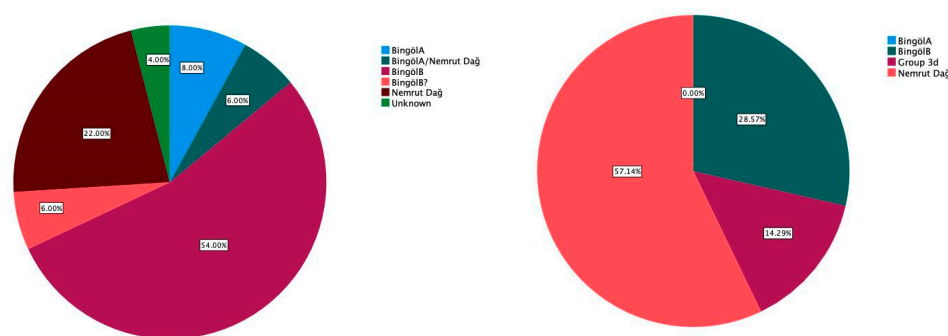

Figure 13. Proportion of main sources at Gre Fılla (PPNB) and Kendale Hecala II (Ubaid period).

Other than Group 3d, the primary sources at Kendale Hecala during the Ubaid period were Bingöl B and Nemrut Dağ. We follow a dramatic shift in obsidian diversity when the available sources at Gre Fılla during PPNB are compared to Kendale Hecala during the Ubaid period. On the other hand, the relative proportion of each source also varied between the two settlements.

7. Conclusions

The lithic industry at Kendale Hecala is significantly dominated by obsidian during the Ubaid period. The proportion of obsidian in the lithic industry is almost twice as much as other knappable siliceous rocks. The lithic analysis reveals obsidian nodules, primary flakes, and production debris, indicating a local work organization, including the reduction and production stages of chaîne opératoire. The three core samples in our study assigned to three different sources may also indicate that the debitage was produced on site, regardless of the raw material type. Therefore, we assume that Kendale Hecala was not connected to a central lithic distribution system. The obsidian as a raw material probably arrived to the site by the local groups (for instance, by transhumance routes) from relatively short distances. Although an exchange and transportation system from a settlement closer to the obsidian source to the vicinity can be expected [45], obsidian artefacts at Kendale Hecala suggest direct contact with raw material prior to the initial stages of obsidian preparation. Except for Group 3d, the distances of the primary sources to Kendale Hecala are approximately 150 km south from Bingöl B and 250 km southwest from Nemrut Dağ [46]. The production activity is in accordance with Kenan Tepe, where the on-site reduction is apparent, although obsidian material constitutes around 18 to 20% of the lithic industry at Kenan Tepe. On the other hand, the long-distance transportation system of obsidian from eastern Anatolia to northwestern Iran, between Lake Urmia and the Lake Van regions, during the Late Neolithic and Chalcolithic periods is also evident from obsidian-sourcing studies [47].

The previous study at Gre Fılla demonstrates a diachronic change in obsidian use in the region. Bingöl A has so far not been detected at Kendale Hecala; therefore, we may assume

that Nemrut Dağ was the main supplier of peralkaline obsidian. The relative dominance of Bingöl B in PPNB at Gre Fılla disappeared at Kendale Hecala, as illustrated in Figure 11. Due to the proximity of the two sites, the continuous chronological sequences, and material culture, it is safe to argue that technological knowledge and cultural information were shared between Gre Fılla (PPNA-PNNB periods) and Kendale Hecala (PN-Ubaid periods). However, future studies will provide more data for identifying the dynamics that affected obsidian procurement at Ambar Çay Valley in the Upper Tigris region between the PPNA and Ubaid periods. On the other hand, the shift in dominant sources and changes in the diversity of raw material between Gre Fılla (PPNB) and Kendale Hecala (Ubaid period) suggest that the distance of the source from the settlement was not the primary factor that influenced the obsidian consumption strategies.

References

1. Carter, R.A.; Philip, G. *Beyond the Ubaid: Transformation and Integration in the Late Prehistoric Societies of the Middle East*; The University of Chicago: Chicago, IL, USA, 2010; pp. 1–23.
2. Porada, E.; Hansen, D.P.; Dunham, S.; Babcock, S.H. The Chronology of Mesopotamia, ca. 7000–1600 BC. In *Chronologies in Old World Archaeology*; Ehrick, R.W., Ed.; University of Chicago Press: Chicago, IL, USA, 1992; pp. 77–121.
3. Lemonnier, P. La description des chaînes opératoires: Contribution à l'analyse des systèmes techniques. *Techniques et Culture* **1976**, *1*, 100–151.
4. Lemonnier, P. *Elements for an Anthropology of Technology*; The University of Michigan: Ann Arbor, MI, USA, 1992; pp. 25–32.
5. Thomalsky, J. Lithic industries of the Ubaid and Post-Ubaid period in northern Mesopotamia. *Publ. L'Institut Français D'Études Anatol.* **2012**, *27*, 417–439.
6. Batist, Z. Obsidian Circulation Networks in Southwest Asia an Anatolia (12,000–5700 B.P.): A Comparative Approach. Master's Thesis, McMaster University, Hamilton, ON, Canada, 2014.
7. Campbell, S.; Healey, E. Diversity in obsidian use in the prehistoric and early historic Middle East. *Quat. Int.* **2018**, *468*, 141–154. [CrossRef]
8. Barge, O.; Kharanaghi, H.A.; Biglari, F.; Moradi, B.; Mashkour, M.; Tengberg, M.; Chataigner, C. Diffusion of Anatolian and Caucasian obsidian in the Zagros Mountains and the highlands of Iran: Elements of explanation in 'least cost path' models. *Quat. Int.* **2018**, *467*, 297–322. [CrossRef]
9. Campbell, S.; Healey, E. Multiple sources: The pXRF analysis of obsidian from Kenan Tepe, SE Turkey. *JAS Rep.* **2016**, *10*, 377–389. [CrossRef]
10. Renfrew, C.; Dixon, J.E.; Cann, J.R. Obsidian and early cultural contact in the Near East. *East. Proc. Prehist. Soc.* **1966**, *32*, 30–37. [CrossRef]
11. Campbell, S.; Healey, E.; Maeda, O. Profiling an unlocated source: Group 3D obsidian in prehistoric and early historic near East. *JAS Rep.* **2020**, *33*, 102533. [CrossRef]
12. Khalidi, L.; Gratuze, B.; Stein, G.; McMahon, A.; Al-Quntar, S.; Carter, R.; Cuttler, R.; Dreshchler, P.; Healey, E.; Inizan, M.L.; et al. The growth of early social networks: New geochemical results of obsidian from the Ubaid to Chalcolithic Period in Syria, Iraq and the Gulf. *JAS Rep.* **2016**, *9*, 743–757. [CrossRef]
13. Muşkara, Ü.; Konak, A. Obsidian source identification at Gre Fılla, Turkey. *JAS Rep.* **2021**, *38*, 103003. [CrossRef]

14. Ökse, A.T. Ambar Dam Salvage Excavations in 2018–2020: Ambar Höyük, Gre Fılla and Kendale Hecala. In *Archaeology of Anatolia Volume IV: Recent Discoveries (2018–2020)*; Sharon, R.S., McMahon, G., Eds.; Cambridge Scholars Press: Newcastle upon Tyne, UK, 2021; pp. 4–20.

15. Ökse, A.T. New Data on the Late Neolithic Pottery from the Northern Upper Tigris Region: Ambar Dam Reservoir. In *Neolithic Pottery from the Near East: Production, Distribution and Use, Proceedings of the 2019 Third International Workshop (Antalya, Turkey)*; Özbal, R., Erdalkıran, M., Tonoike, Y., Eds.; Koç University Press: Istanbul, Turkey, 2020; Volume 259, pp. 301–322.

16. Davis, M.K.; Jackson, T.L.; Shackley, M.S.; Teague, T.; Hampel, J.H. Factors affecting the energy-dispersive X-ray fluorescence (EDXRF) analysis of archaeological obsidian. In *Archaeological Obsidian Studies: Method and Theory*; Shackley, M.S., Ed.; Plenum Press: New York, NY, USA, 1998; pp. 159–180.

17. Shackley, M.S. An introduction to X-ray fluorescence (XRF) analysis in archaeology. In *X-ray Fluorescence Spectrometry (XRF) in Geoarchaeology*; Shackley, M.S., Ed.; Springer: New York, NY, USA, 2011; pp. 7–44.

18. Gauvin, R.; Lifshin, E. Simulation of X-ray emission from rough surfaces. *Microchim. Acta* **2000**, *132*, 201–204. [CrossRef]

19. Liritsiz, I.; Zacharias, N. Portable XRF of Archaeological Artifacts: Current Research, Potentials and Limitations. In *X-ray Fluorescence Spectrometry (XRF) in Geoarchaeology*; Shackley, M.S., Ed.; Springer: New York, NY, USA, 2011; pp. 1009–1142.

20. Steiner, A.E.; Conrey, R.M.; Wolff, J.A. PXRF calibrations for volcanic rocks and the application of in-field analysis to the geosciences. *Chem. Geol.* **2017**, *453*, 35–54. [CrossRef]

21. Hunt, A.M.; Speakman, R.J. Portable XRF analysis of archaeological sediments and ceramics. *JAS* **2015**, *53*, 626–638. [CrossRef]

22. Ferguson, J.R. *X-ray Fluorescence of Obsidian: Approaches to Calibration and the Analysis of Small Samples. Handheld XRF for Art and Archaeology*; Leuven University Press: Leuven, Belgium, 2012; pp. 401–422.

23. Nazaroff, A.J.; Prufer, K.M.; Drake, B.L. Assessing the applicability of portable X-ray fluorescence spectrometry for obsidian provenance research in the Maya lowlands. *JAS* **2010**, *37*, 885–895. [CrossRef]

24. Frahm, E. Validity of "off-the-shelf" handheld portable XRF for sourcing Near Eastern obsidian chip debris. *JAS* **2013**, *40*, 1080–1092. [CrossRef]

25. Glascock, M.D.; Neff, H. Neutron activation analysis and provenance research in archaeology. *Meas. Sci. Technol.* **2003**, *14*, 1516–1526. [CrossRef]

26. Grave, P.; Kealhofer, L.; Marsh, B.; Gates, M.H. Using neutron activation analysis to identify scales of interaction at Kinet Höyük, Turkey. *JAS* **2008**, *35*, 1974–1992. [CrossRef]

27. Forster, N.; Grave, P. Non-destructive PXRF analysis of museum-curated obsidian from the Near East. *JAS* **2012**, *35*, 1974–1992. [CrossRef]

28. Prokeš, L.; Galiová, M.V.; Hušková, S.; Vaculovič, T.; Hrdlička, A.; Mason, A.Z.; Neff, H.; Přichystal, A.; Kanický, V. Laser microsampling and multivariate methods in provenance studies of obsidian artefacts. *Chem. Pap.* **2015**, *69*, 761–778. [CrossRef]

29. Robin, A.K.; Mouralis, D.; Akköprü, E.; Gratuze, B.; Kuzucuoğlu, C.; Nomade, S.; Pereira, A.; Doğu, A.F.; Erturaç, K.; Khalidi, L. Identification and characterization of two new obsidian sub-sources in the Nemrut volcano (Eastern Anatolia, Turkey): The Sıcaksu and Kayacık obsidian. *JAS Rep.* **2016**, *9*, 705–717. [CrossRef]

30. Orange, M.; Carter, T.; Le Bourdonnec, F.X. Sourcing obsidian from Tell Aswad and Qdeir 1 (Syria) by SEM-EDS and EDXRF: Methodological implications. *Comptes Rendus Palevol* **2013**, *12*, 173–180. [CrossRef]

31. Baxter, M.J.; Buck, C.E. Data Handling and Statistical Analysis. In *Modern Analytical Methods in Art and Archaeology*; Ciliberto, E., Spoto, G., Eds.; John Wiley and Sons: New York, NY, USA, 2000; pp. 681–746.

32. Glascock, D.M. A systematic approach to geochemical sourcing of obsidian artifacts. *Sci. Cult.* **2020**, *2*, 35–47.

33. Liritzis, I.; Xanthopoulou, V.; Palamara, E.; Papageorgiou, I.; Iliopoulos, I.; Zacharias, N.; Vafiadou, A.; Karydas, A.G. Characterization and provenance of ceramic artifacts and local clays from Late Mycenaean Kastrouli (Greece) by means of p-XRF screening and statistical analysis. *J. Cult. Herit.* **2020**, *46*, 61–81. [CrossRef]

34. López-García, P.A.; Vidal-Aldana, C.I.; Gómez-Ambríz, E.A.; Argote, D.L. The obsidian of la ferrería site: Local consumption and long-distance interactions in north and northwestern Mexico. *JAS Rep.* **2021**, *9*, 103081. [CrossRef]

35. Chataigner, C.; Poidevin, J.L.; Arnaud, N.O. Turkish occurrences of obsidian and use by prehistoric peoples in the Near East from 14,000 to 6000 BP. *J. Volcanol. Geotherm. Res.* **1998**, *85*, 517–537. [CrossRef]

36. Chabot, J.; Poidevin, J.L.; Chataigner, C.; Fortin, M. Caracterisation et provenance des artefacts en obsidienne de Tell'Atij et de Tell Gudeda (III millenaire, Syrie). *Cahiers d'Acheologie Du CELAT* **2001**, *10*, 241–256.

37. Francaviglia, V.M. L'origine des outils en obsidienne de Tell Magzalia, Tell Sotto, Yarim Tepe et Kül Tepe, Iraq. *Paléorient* **1994**, *20*, 18–31. [CrossRef]

38. Gratuze, B. Obsidian characterization by laser ablation ICP-MS and its application to prehistoric trade in the Mediterranean and the Near East: Sources and distribution of obsidian within the Aegean and Anatolia. *JAS* **1999**, *26*, 869–881. [CrossRef]

39. Bressy, C.; Poupeau, G.; Yener, K.A. Cultural interactions during the Ubaid and Halaf periods: Tell Kurdu (Amuq Valley, Turkey) obsidian sourcing. *JAS* **2005**, *32*, 1560–1565. [CrossRef]

40. Khalidi, L.; Gratuze, B.; Boucetta, S. Provenance of obsidian excavated from Late Chalcolithic levels at the sites of Tell Hamoukar and Tell Brak, Syria. *Archaeometry* **2009**, *51*, 879–893. [CrossRef]

41. Poupeau, G.; Le Bourdonnec, F.X.; Carter, T.; Delerue, S.; Shackley, M.S.; Barrat, J.A.; Dubernet, S.; Moretto, P.; Calligaro, T.; Milić, M.; et al. The use of SEM-EDS, PIXE and EDXRF for obsidian provenance studies in the Near East: A case study from Neolithic Çatalhöyük (central Anatolia). *JAS* **2010**, *37*, 2705–2720. [CrossRef]

42. Chataigner, C. Les propriétés géochimiques des obsidiennes et la distinction des sources de Bingöl et du Nemrut Dag. *Paléorient* **1994**, *20*, 9–17. [CrossRef]
43. Frahm, E. Distinguishing Nemrut Dağ and Bingöl A obsidians: Geochemical and landscape differences and the archaeological implications. *JAS* **2012**, *39*, 1436–1444. [CrossRef]
44. Frahm, E. Variation in Nemrut Dağ obsidian at Pre-Pottery Neolithic to Late Bronze Age sites (or: All that's Nemrut Dağ obsidian isn't the Sıcaksu source). *JAS* **2020**, *32*, 102438. [CrossRef]
45. Abedi, A.; Vosough, B.; Razani, M.; Kasiri, M.B.; Steimiger, D.; Ebrahimi, G. Obsidian Deposits from Northwestern Iran and First Analytical Results: Implications for Prehistoric Production and Trade. *Mediterr. Archaeol. Archaeom.* **2018**, *18*, 107–118.
46. Ökse, A.T. Yukarı Dicle Havzasında Ambar Çayı Vadisi Yerleşim Tarihi. *Olba* **2020**, *28*, 1–34.
47. Abedi, A.; Varoutsikos, B.; Chataigner, C. Provenance of obsidian artifacts from the Chalcolithic site of Dava Göz in NW IRAN using portable XRF. *JAS Rep.* **2018**, *20*, 756–767. [CrossRef]